Electronic Supplementary Material (ESI) for Journal of Materials Chemistry C.


# Supporting information

# The luminescent sensing profiles based on anion-responsive lanthanide(III) quinolinecarboxylate materials: solid-state structures, photophysical properties, and anionic species recognition

Wentao Xu,[a] Youfu Zhou,*[a] Decai Huang,[a] Mingyi Su,[ab] Kun Wang,[ab] Ming Xiang,[ab] and Maochun Hong[a]

[a] Key Laboratory of Optoelectronic Materials Chemistry and Physics, Fujian Institute of Research on the Structure of Matter, Chinese Academy of Sciences, Fuzhou, 350002,China

[b] University of the Chinese Academy of Sciences, Beijing, 100049, China

**Table S1**. Crystallographic data and refinements for **2**–**5**

| | **2** | **3** | **4** | **5** |
|---|---|---|---|---|
| Formula | $C_{54}H_{48}N_3O_9Pr$ | $C_{54}H_{48}N_3O_9Nd$ | $C_{54}H_{48}N_3O_9Sm$ | $C_{54}H_{48}N_3O_9Eu$ |
| Formula weight | 1023.86 | 1027.19 | 1033.30 | 1034.91 |
| Crystal system | triclinic | triclinic | triclinic | triclinic |
| Space group | *P*-1 | *P*-1 | *P*-1 | *P*-1 |
| *a* (Å) | 11.9877(3) | 11.9730(2) | 11.9586(3) | 11.9567(5) |
| *b* (Å) | 12.8636(5) | 12.8879(5) | 12.8019(4) | 12.8560(5) |
| *c* (Å) | 15.9294(6) | 15.9094(6) | 15.9246(5) | 15.8977(6) |
| $\alpha$(°) | 86.856(3) | 87.030(7) | 87.217(3) | 87.548(3) |
| $\beta$(°) | 73.942(3) | 73.854(6) | 74.158(2) | 74.215(4) |
| $\gamma$(°) | 83.926(3) | 83.803(7) | 83.990(2) | 83.653(3) |
| Volume(Å$^3$) | 2346.46(14) | 2343.71(13) | 2331.95(12) | 2336.9 (2) |
| *T* (K) | 100(18) | 293(2) | 100.0(3) | 100(15) |
| *Z* | 2 | 2 | 2 | 2 |
| $D_c$ (g·cm$^{-3}$) | 1.449 | 1.456 | 1.472 | 1.471 |
| $\mu$(mm$^{-1}$) | 8.467 | 1.169 | 9.961 | 10.111 |
| *F*(000) | 1048 | 1050 | 1054 | 1056 |
| $R_{int}$ | 0.0222 | 0.0593 | 0.0349 | 0.0445 |
| $R_1$[a]/$wR_2$[b] [$I>2\sigma(I)$] | 0.0331/ 0.0864 | 0.0437/ 0.1121 | 0.0341/ 0.0866 | 0.0504/0.1374 |
| $R_1$/$wR_2$ (all data) | 0.0361/0.0888 | 0.0487/ 0.1169 | 0.0406/ 0.0905 | 0.0560/0.1406 |
| GOF | 1.052 | 1.116 | 1.062 | 1.106 |

[a] $R_1 = \sum\|F_o\| - \|F_c\|/\sum|F_o|$; [b] $wR_2 = \sum[w(F_o^2 - F_c^2)^2]/\sum[w(F_o^2)^2]^{1/2}$.

**Table S2**. Selected bond lengths (Å) and bond angles (°) for **2**−**5**

| **Complex 2** | | | |
|---|---|---|---|
| Bond | Dist.( Å) | Bond | Dist.( Å) |
| Pr(1)-O(6)#1 | 2.428(2) | Pr(1)-O(4) | 2.566(2) |
| Pr(1)-O(1)#1 | 2.431(2) | Pr(1)-O(2) | 2.568(2) |
| Pr(1)-O(5) | 2.472(2) | Pr(1)-O(1) | 2.613(2) |
| Pr(1)-O(7) | 2.482(2) | O(1)-Pr(1)#1 | 2.431(2) |
| Pr(1)-O(3) | 2.511(2) | O(6)-Pr(1)#1 | 2.428(2) |
| Pr(1)-O(8) | 2.559(2) | | |
| | | | |
| Angle | (°) | Angle | (°) |
| O(6)#1-Pr(1)-O(1)#1 | 71.51(7) | O(7)-Pr(1)-O(4) | 100.13(8) |
| O(6)#1-Pr(1)-O(5) | 134.81(7) | O(3)-Pr(1)-O(4) | 51.18(8) |
| O(1)#1-Pr(1)-O(5) | 74.00(7) | O(8)-Pr(1)-O(4) | 76.10(9) |
| O(6)#1-Pr(1)-O(7) | 144.12(7) | O(6)#1-Pr(1)-O(2) | 81.67(8) |
| O(1)#1-Pr(1)-O(7) | 143.92(7) | O(1)#1-Pr(1)-O(2) | 119.67(7) |
| O(5)-Pr(1)-O(7) | 72.48(7) | O(5)-Pr(1)-O(2) | 91.03(8) |
| O(6)#1-Pr(1)-O(3) | 127.22(8) | O(7)-Pr(1)-O(2) | 74.01(8) |
| O(1)#1-Pr(1)-O(3) | 76.86(8) | O(3)-Pr(1)-O(2) | 151.08(8) |
| O(5)-Pr(1)-O(3) | 69.89(7) | O(8)-Pr(1)-O(2) | 69.07(9) |
| O(7)-Pr(1)-O(3) | 79.46(8) | O(4)-Pr(1)-O(2) | 145.02(8) |
| O(6)#1-Pr(1)-O(8) | 72.33(8) | O(6)#1-Pr(1)-O(1) | 72.38(7) |
| O(1)#1-Pr(1)-O(8) | 140.64(8) | O(1)#1-Pr(1)-O(1) | 70.10(8) |
| O(5)-Pr(1)-O(8) | 145.08(8) | O(5)-Pr(1)-O(1) | 68.99(7) |
| O(7)-Pr(1)-O(8) | 74.50(8) | O(7)-Pr(1)-O(1) | 109.00(7) |
| O(3)-Pr(1)-O(8) | 114.64(9) | O(3)-Pr(1)-O(1) | 132.62(7) |
| O(6)#1-Pr(1)-O(4) | 84.90(8) | O(8)-Pr(1)-O(1) | 112.48(8) |
| O(1)#1-Pr(1)-O(4) | 85.72(8) | O(4)-Pr(1)-O(1) | 150.85(8) |
| O(5)-Pr(1)-O(4) | 120.66(8) | O(2)-Pr(1)-O(1) | 50.30(7) |
| Symmetry codes: (#1) -x+2,-y+1,-z | | | |

**Complex 3**

| Bond | Dist.( Å) | Bond | Dist.( Å) |
|---|---|---|---|
| Nd(1)-O(5) | 2.411(3) | Nd(1)-O(1) | 2.543(3) |
| Nd(1)-O(4)#1 | 2.414(3) | Nd(1)-O(3) | 2.557(3) |
| Nd(1)-O(6)#1 | 2.454(3) | Nd(1)-O(4) | 2.591(3) |
| Nd(1)-O(8) | 2.469(3) | O(4)-Nd(1)#1 | 2.414(3) |
| Nd(1)-O(2) | 2.493(3) | O(6)-Nd(1)#1 | 2.454(3) |
| Nd(1)-O(7) | 2.541(4) | | |

| Angle | (°) | Angle | (°) |
|---|---|---|---|
| O(5)-Nd(1)-O(4)#1 | 71.72(10) | O(8)-Nd(1)-O(1) | 100.53(11) |
| O(5)-Nd(1)-O(6)#1 | 135.23(10) | O(2)-Nd(1)-O(1) | 51.32(11) |
| O(4)#1-Nd(1)-O(6)#1 | 74.02(9) | O(7)-Nd(1)-O(1) | 75.47(13) |
| O(5)-Nd(1)-O(8) | 143.97(10) | O(5)-Nd(1)-O(3) | 81.77(11) |
| O(4)#1-Nd(1)-O(8) | 143.92(9) | O(4)#1-Nd(1)-O(3) | 120.00(10) |
| O(6)#1-Nd(1)-O(8) | 72.47(9) | O(6)#1-Nd(1)-O(3) | 91.35(11) |
| O(5)-Nd(1)-O(2) | 127.10(10) | O(8)-Nd(1)-O(3) | 73.95(10) |
| O(4)#1-Nd(1)-O(2) | 77.22(10) | O(2)-Nd(1)-O(3) | 151.03(11) |
| O(6)#1-Nd(1)-O(2) | 70.14(10) | O(7)-Nd(1)-O(3) | 69.32(13) |
| O(8)-Nd(1)-O(2) | 79.17(10) | O(1)-Nd(1)-O(3) | 144.54(12) |
| O(5)-Nd(1)-O(7) | 72.80(11) | O(5)-Nd(1)-O(4) | 72.49(9) |
| O(4)#1-Nd(1)-O(7) | 141.09(10) | O(4)#1-Nd(1)-O(4) | 70.11(10) |
| O(6)#1-Nd(1)-O(7) | 144.74(10) | O(6)#1-Nd(1)-O(4) | 69.29(9) |
| O(8)-Nd(1)-O(7) | 73.89(10) | O(8)-Nd(1)-O(4) | 109.23(10) |
| O(2)-Nd(1)-O(7) | 113.31(13) | O(2)-Nd(1)-O(4) | 133.23(10) |
| O(5)-Nd(1)-O(1) | 84.07(11) | O(7)-Nd(1)-O(4) | 113.19(12) |
| O(4)#1-Nd(1)-O(1) | 85.46(10) | O(1)-Nd(1)-O(4) | 150.23(10) |
| O(6)#1-Nd(1)-O(1) | 120.96(10) | O(3)-Nd(1)-O(4) | 50.61(10) |

Symmetry codes: (#1) -x+1,-y+2,-z

**Complex 4**

| Bond | Dist.( Å) | Bond | Dist.( Å) |
|---|---|---|---|
| Sm(1)-O(4)#1 | 2.381(2) | Sm(1)-O(3) | 2.512(3) |
| Sm(1)-O(6)#1 | 2.389(2) | Sm(1)-O(2) | 2.519(3) |
| Sm(1)-O(5) | 2.423(2) | Sm(1)-O(4) | 2.591(2) |
| Sm(1)-O(8) | 2.436(2) | O(4)-Sm(1)#1 | 2.381(2) |
| Sm(1)-O(1) | 2.468(2) | O(6)-Sm(1)#1 | 2.389(2) |
| Sm(1)-O(7) | 2.505(3) | | |

| Angle | (°) | Angle | (°) |
|---|---|---|---|
| O(4)#1-Sm(1)-O(6)#1 | 72.35(8) | O(8)-Sm(1)-O(3) | 74.16(9) |
| O(4)#1-Sm(1)-O(5) | 74.28(8) | O(1)-Sm(1)-O(3) | 149.29(9) |
| O(6)#1-Sm(1)-O(5) | 135.43(8) | O(7)-Sm(1)-O(3) | 69.79(9) |
| O(4)#1-Sm(1)-O(8) | 143.27(8) | O(4)#1-Sm(1)-O(2) | 85.74(8) |
| O(6)#1-Sm(1)-O(8) | 144.22(8) | O(6)#1-Sm(1)-O(2) | 83.73(8) |
| O(5)-Sm(1)-O(8) | 72.43(8) | O(5)-Sm(1)-O(2) | 122.23(8) |
| O(4)#1-Sm(1)-O(1) | 76.93(9) | O(8)-Sm(1)-O(2) | 99.14(9) |
| O(6)#1-Sm(1)-O(1) | 127.57(9) | O(1)-Sm(1)-O(2) | 52.23(8) |
| O(5)-Sm(1)-O(1) | 70.44(8) | O(7)-Sm(1)-O(2) | 75.06(9) |
| O(8)-Sm(1)-O(1) | 77.70(9) | O(3)-Sm(1)-O(2) | 144.74(9) |
| O(4)#1-Sm(1)-O(7) | 140.98(8) | O(4)#1-Sm(1)-O(4) | 70.10(9) |
| O(6)#1-Sm(1)-O(7) | 72.02(9) | O(6)#1-Sm(1)-O(4) | 72.09(8) |
| O(5)-Sm(1)-O(7) | 144.51(9) | O(5)-Sm(1)-O(4) | 69.28(8) |
| O(8)-Sm(1)-O(7) | 74.33(9) | O(8)-Sm(1)-O(4) | 111.05(8) |
| O(1)-Sm(1)-O(7) | 113.92(9) | O(1)-Sm(1)-O(4) | 133.20(8) |
| O(4)#1-Sm(1)-O(3) | 120.63(8) | O(7)-Sm(1)-O(4) | 112.64(9) |
| O(6)#1-Sm(1)-O(3) | 83.07(9) | O(3)-Sm(1)-O(4) | 50.91(8) |
| O(5)-Sm(1)-O(3) | 89.36(9) | O(2)-Sm(1)-O(4) | 149.81(8) |

Symmetry codes: (#1) -x+2,-y,-z

**Complex 5**

| Bond | Dist.( Å) | Bond | Dist.( Å) |
|---|---|---|---|
| Eu(1)-O(5) | 2.366(3) | Eu(1)-O(4) | 2.498(4) |
| Eu(1)-O(2)#1 | 2.368(4) | Eu(1)-O(8) | 2.496(4) |
| Eu(1)-O(6)#1 | 2.416(3) | Eu(1)-O(2) | 2.576(3) |
| Eu(1)-O(7) | 2.421(4) | O(2)-Eu(1)#1 | 2.368(4) |
| Eu(1)-O(3) | 2.456(4) | O(6)-Eu(1)#1 | 2.416(3) |
| Eu(1)-O(1) | 2.492(4) | | |

| Angle | (°) | Angle | (°) |
|---|---|---|---|
| O(5)-Eu(1)-O(2)#1 | 72.54(12) | O(7)-Eu(1)-O(4) | 99.46(14) |
| O(5)-Eu(1)-O(6)#1 | 135.69(12) | O(3)-Eu(1)-O(4) | 52.34(13) |
| O(2)#1-Eu(1)-O(6)#1 | 74.40(12) | O(1)-Eu(1)-O(4) | 144.84(14) |
| O(5)-Eu(1)-O(7) | 143.97(12) | O(5)-Eu(1)-O(8) | 72.08(14) |
| O(2)#1-Eu(1)-O(7) | 143.36(12) | O(2)#1-Eu(1)-O(8) | 141.08(13) |
| O(6)#1-Eu(1)-O(7) | 72.50(12) | O(6)#1-Eu(1)-O(8) | 144.33(13) |
| O(5)-Eu(1)-O(3) | 127.57(13) | O(7)-Eu(1)-O(8) | 74.00(13) |
| O(2)#1-Eu(1)-O(3) | 76.89(13) | O(3)-Eu(1)-O(8) | 113.56(16) |
| O(6)#1-Eu(1)-O(3) | 70.50(12) | O(1)-Eu(1)-O(8) | 69.90(15) |
| O(7)-Eu(1)-O(3) | 77.63(13) | O(4)-Eu(1)-O(8) | 75.07(16) |
| O(5)-Eu(1)-O(1) | 83.30(14) | O(5)-Eu(1)-O(2) | 72.25(12) |
| O(2)#1-Eu(1)-O(1) | 120.99(12) | O(2)#1-Eu(1)-O(2) | 70.14(14) |
| O(6)#1-Eu(1)-O(1) | 89.26(13) | O(6)#1-Eu(1)-O(2) | 69.27(11) |
| O(7)-Eu(1)-O(1) | 73.95(13) | O(7)-Eu(1)-O(2) | 111.24(12) |
| O(3)-Eu(1)-O(1) | 149.04(14) | O(3)-Eu(1)-O(2) | 133.20(13) |
| O(5)-Eu(1)-O(4) | 83.27(13) | O(1)-Eu(1)-O(2) | 51.21(12) |
| O(2)#1-Eu(1)-O(4) | 85.23(13) | O(4)-Eu(1)-O(2) | 149.30(13) |
| O(6)#1-Eu(1)-O(4) | 122.34(13) | O(8)-Eu(1)-O(2) | 113.00(14) |

Symmetry codes: (#1) -x+1,-y+1,-z+1

**Table S3** The calculated energy and interaction energy about $HSO_4^-/H_2PO_4^-$ with ligand by DFT method at B3LYP-D3/6-31++G* level,

| | $HSO_4$-L | $H_2PO_4$-L |
|---|---|---|
| E($HSO_4/H_2PO_4$-L) (a.u.) | -1521.38928 | -1465.30232 |
| E(L) (a.u.) | -821.63408 | |
| E($HSO_4^-/H_2PO_4^-$) (a.u.) | -699.73284 | -643.64658 |
| E($HSO_4/H_2PO_4$^L) (kcal/mol) | -3.35569 | -3.25048 |

1 a.u.=627.51 kJ/mol = 150.05 kcal/mol, E($HSO_4/H_2PO_4$^L)=E($HSO_4/H_2PO_4$-L)- E($HSO_4^-/H_2PO_4^-$) - E(L)

**Table S4** calculated hydrogen bond length between $HSO_4^-/H_2PO_4^-$ and PQC

| | C-H | C-H…O | H…O | O-H | O-H…N | H…N |
|---|---|---|---|---|---|---|
| L | 1.08499 | | | | | |
| $HSO_4^-$ | | | | 0.96931 | | |
| $HSO_4$-L | 1.09065 | 3.14557 | 2.05772 | 0.98225 | 2.95102 | 1.96891 |
| $H_2PO_4^-$ | | | | 0.96638 | | |
| $H_2PO_4$-L | 1.09562 | 3.07134 | 1.97948 | 0.97669 | 2.99027 | 2.01643 |

**Table S5** The calculated energy and interaction energy about $HSO_4^-/H_2PO_4^-$ with $Eu^{3+}$ in monodentate mode by DFT method at B3LYP/6-31G**(ECP52MWB) level

| | $Eu(HSO_4)_3(H_2O)_5$ | $Eu(H_2PO_4)_3(H_2O)_5$ |
|---|---|---|
| E($Eu^{3+}$) (a.u.) | -33.81557 | |
| E($H_2O$) (a.u.) | -76.41974 | |
| E($HSO_4/H_2PO_4$) (a.u.) | -699.69269 | -643.59804 |
| E[$Eu(HSO_4/H_2PO_4)_3(H_2O)_5$] (a.u.) | -2516.73106 | -2348.53679 |
| E($H_2O$^$Eu^{3+}$) (a.u.) | -0.11017 | |
| E($HSO_4/H_2PO_4$^$Eu^{3+}$) (kcal/mol) | -59.16024 | -63.62655 |

**Table S6** The calculated energy and interaction energy about $HSO_4^-/H_2PO_4^-$/L with $Eu^{3+}$ in bidentate mode by DFT method at B3LYP/6-31G**(ECP52MWB) level

| | $Eu(HSO_4)_3(H_2O)_2$ | $Eu(H_2PO_4)_3(H_2O)_2$ | $Eu(L)_3(H_2O)_2$ |
|---|---|---|---|
| E($Eu^{3+}$) (a.u.) | -33.81557 | | |
| E($H_2O$) (a.u.) | -76.41974 | | |
| E($HSO_4/H_2PO_4$/L) (a.u.) | -699.69269 | -643.59804 | -821.02425 |
| E[$Eu(HSO_4/H_2PO_4/L)_3(H_2O)_2$] (a.u.) | -2287.37066 | -2119.17105 | -2651.38530 |
| E($H_2O$^$Eu^{3+}$) (a.u.) | -0.11017 | | |
| E($HSO_4/H_2PO_4$/L^$Eu^{3+}$) (kcal/mol) | -70.58065 | -74.78070 | -71.57474 |

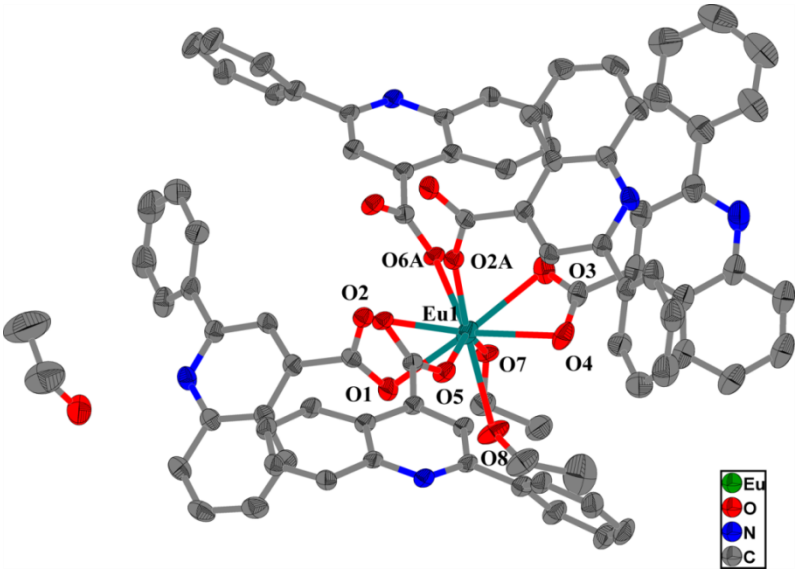


**Fig. S1** The coordination environment around Eu(III) in **$Eu_2PQC_6$** with the thermal ellipsoid at the 30% probability level. Symmetry codes: A: 1-x, 1-y, 1-z.

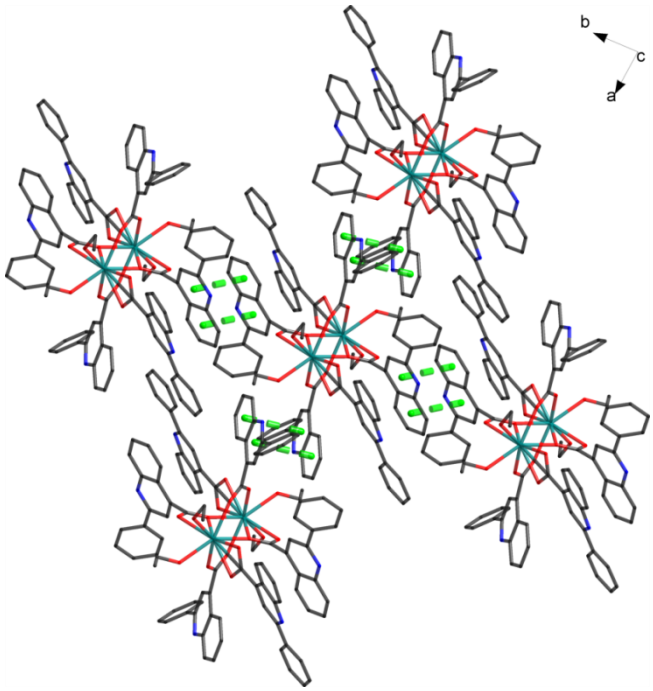


**Fig. S2** 3D framework of **$Eu_2PQC_6$** propagates through the π···π interactions (denoted by the green dotted lines) with the intercentroid distances being 3.621 Å and 3.493 Å respectively.

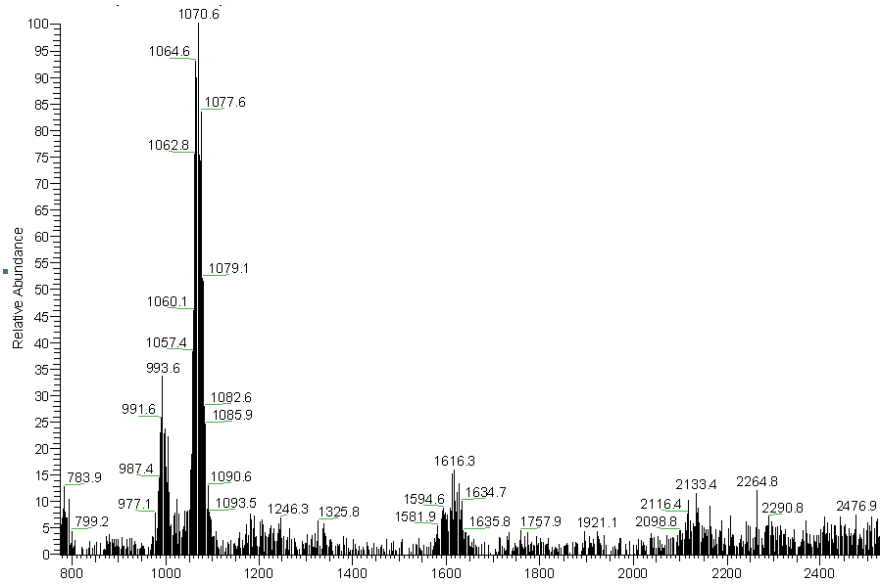


**Fig. S3** Mass spectral analysis of [$\mathbf{Eu_2PQC_6}$+4$H_2O$] complex.

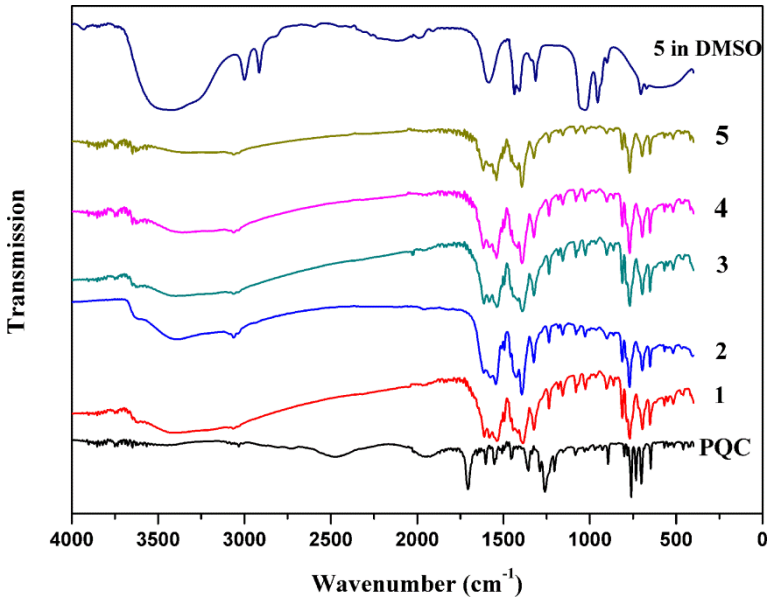


**Fig. S4** IR spectra of PQC ligand, complex **1-5** in solid state and **5** in solution.

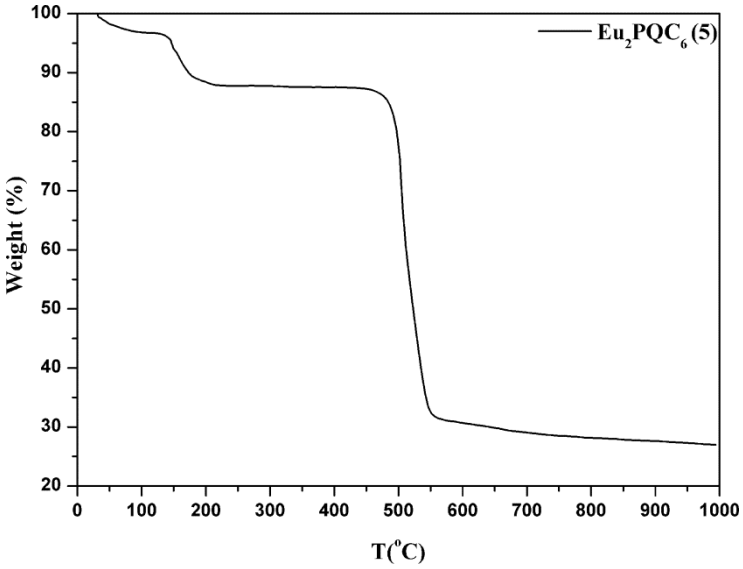


**Fig. S5** TGA diagram of **5** under $N_2$ atmosphere.

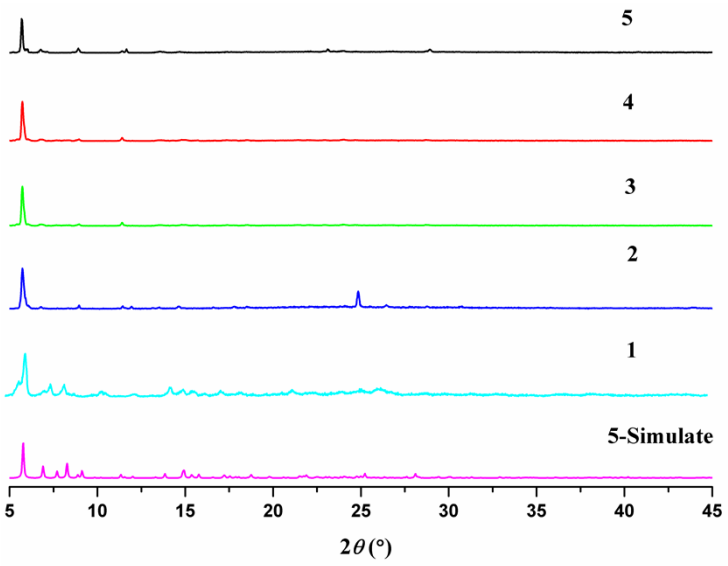


**Fig. S6** PXRD diagram of **1-5**.

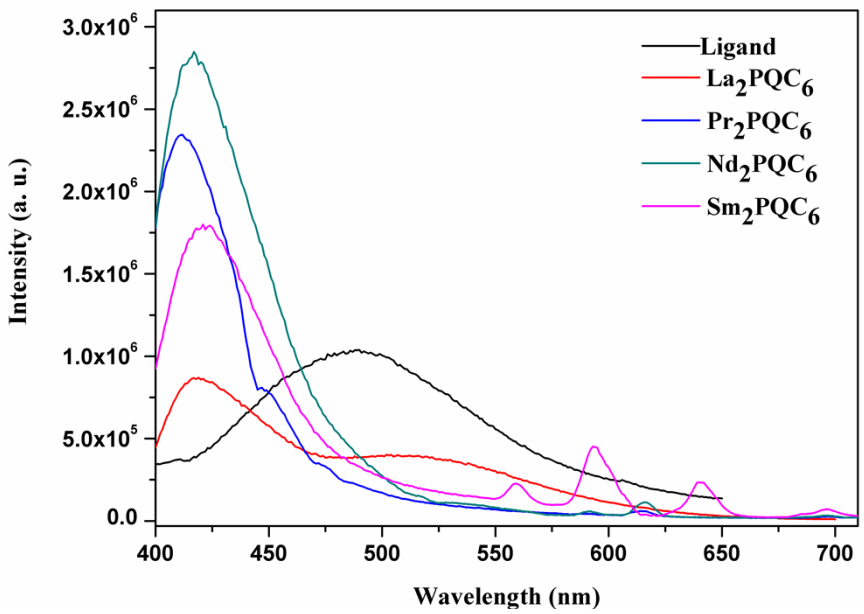


**Fig. S7** Room-temperature emission spectra of ligand and complexes **1-4** ($\lambda_{ex}$ = 345 nm).

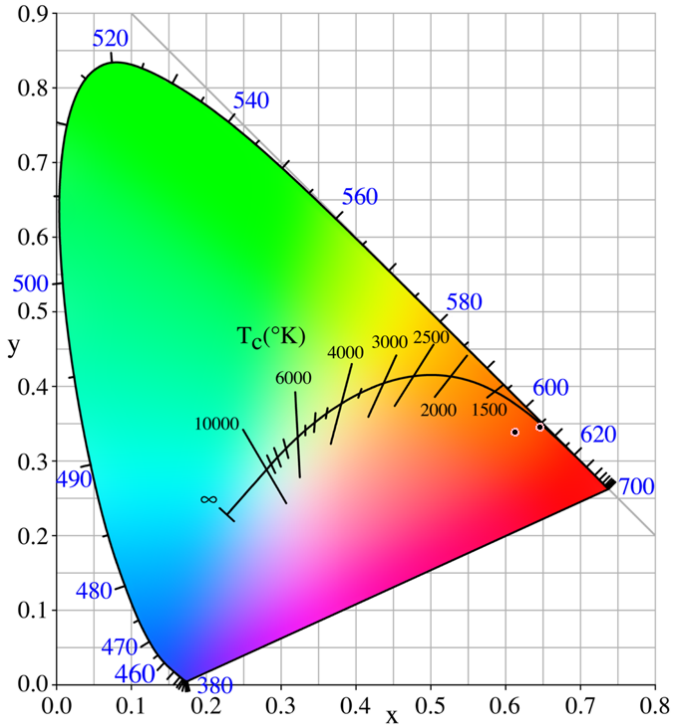


**Fig. S8** The CIE chromaticity coordinates of $\mathbf{Eu_2PQC_6}$ in solid state and solution.

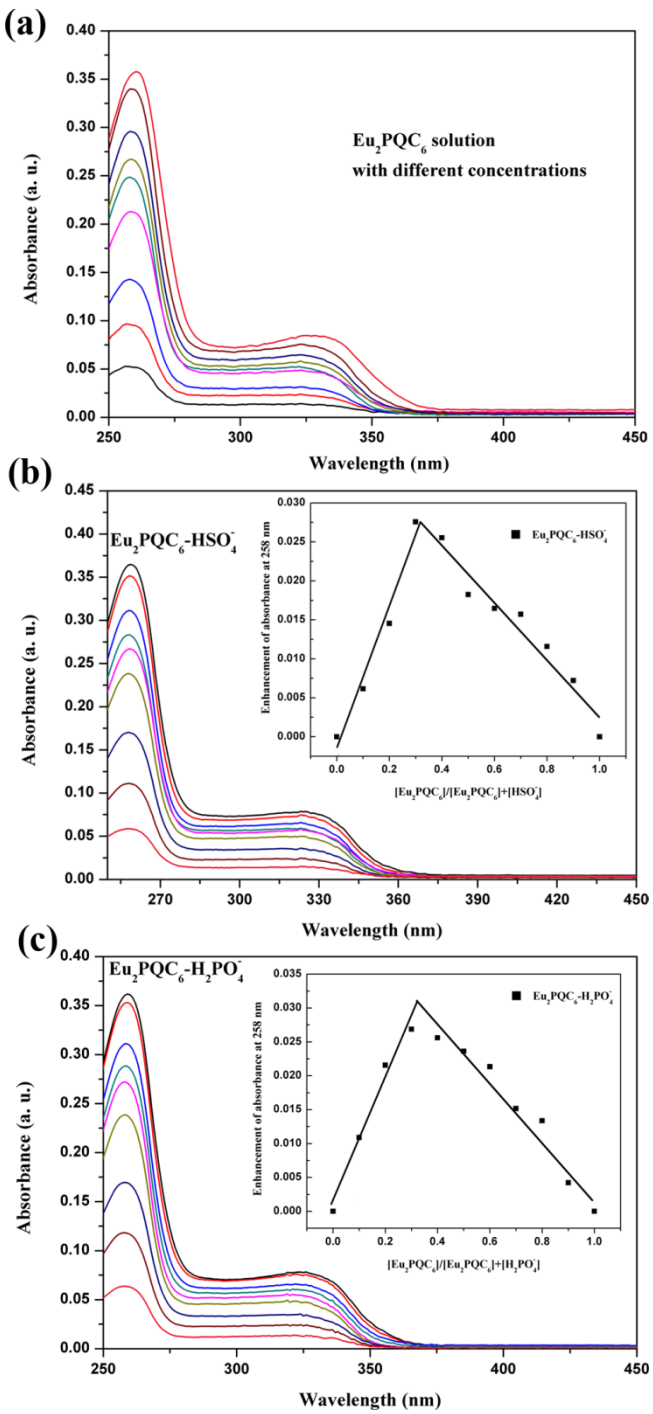


**Fig. S9** Fluorescence emission spectra of (a) **$Eu_2PQC_6$** solution with different concentrations as calibration, (b) **$Eu_2PQC_6$**-$HSO_4^-$ solution with different mol fractions, (c) **$Eu_2PQC_6$**-$H_2PO_4^-$ solution with different mol fractions. The insets in the upper-right show Job's plots after calibration for the determination of the stoichiometry of **$Eu_2PQC_6$** to $HSO_4^-$/ $H_2PO_4^-$.

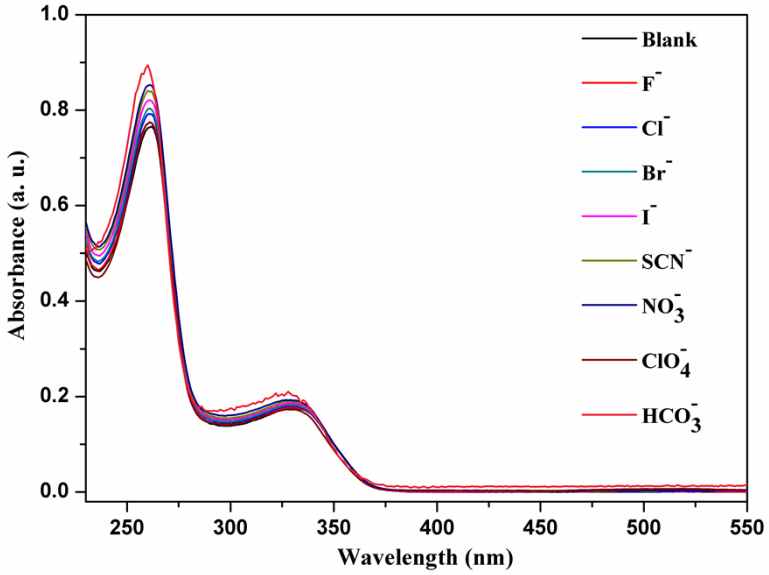


**Fig. S10** The UV-vis absorption spectra of **5** (5μM) in ETOH solution upon addition of $F^-$, $Cl^-$, $Br^-$, $I^-$, $NO_3^-$, $ClO_4^-$, $SCN^-$ and $HCO_3^-$ anions (6.0 equiv).

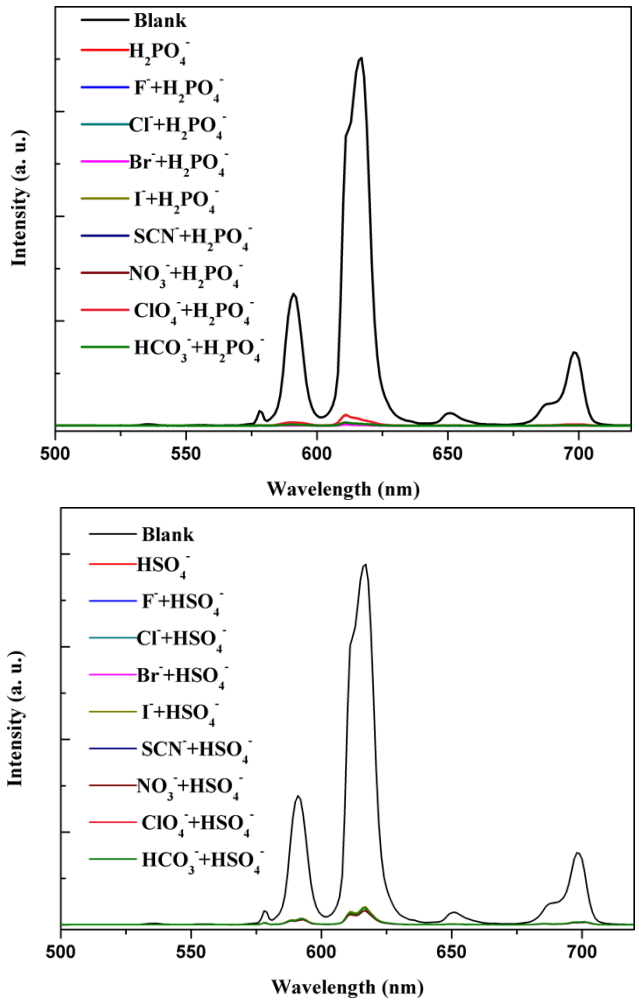


**Fig. S11** Fluorescence of $\mathbf{Eu_2PQC_6}$ in EtOH–DMSO (95:5 v/v) solution (16.7 μM) under $\lambda_{ex}$ = 343 nm and its complexation with $H_2PO_4^-$ and $HSO_4^-$ (3 equiv) in the presence of different anions (6 equiv).

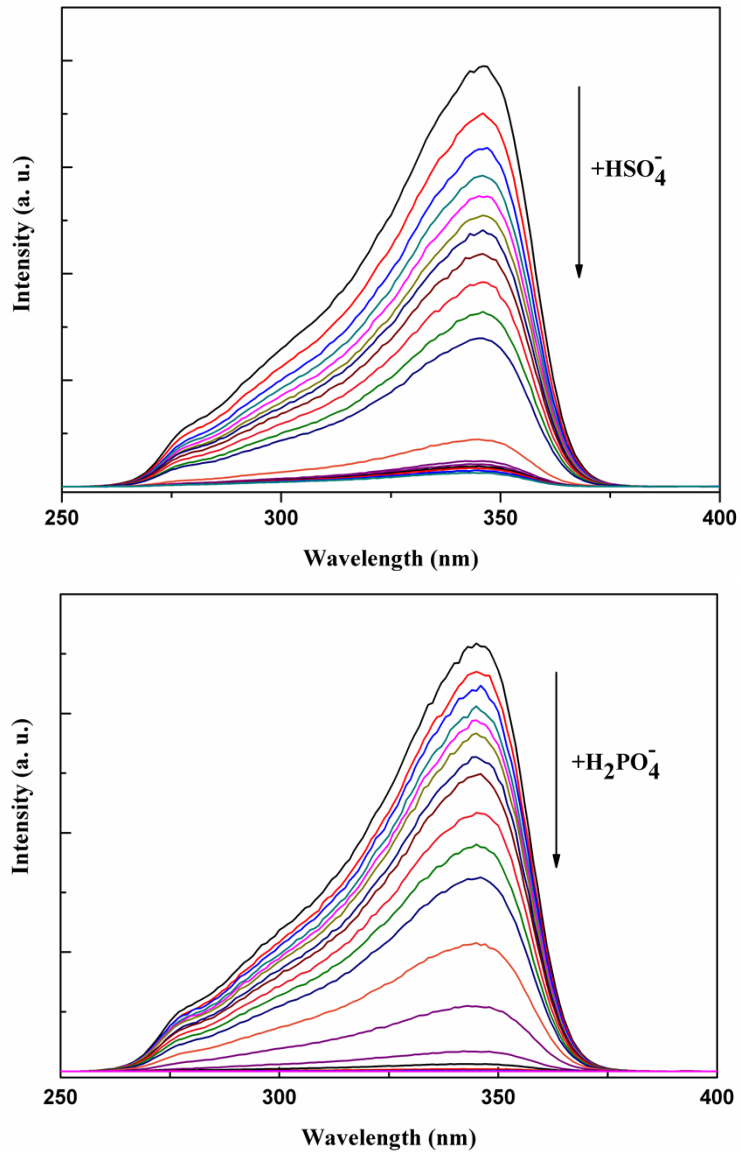


**Fig. S12** The changes in the excitation spectra of **$Eu_2PQC_6$** (16.7 μM) in ETOH-DMSO (v/v = 95:5) solution upon addition of $H_2PO_4^-$ and $HSO_4^-$ (0 – 22 equiv).

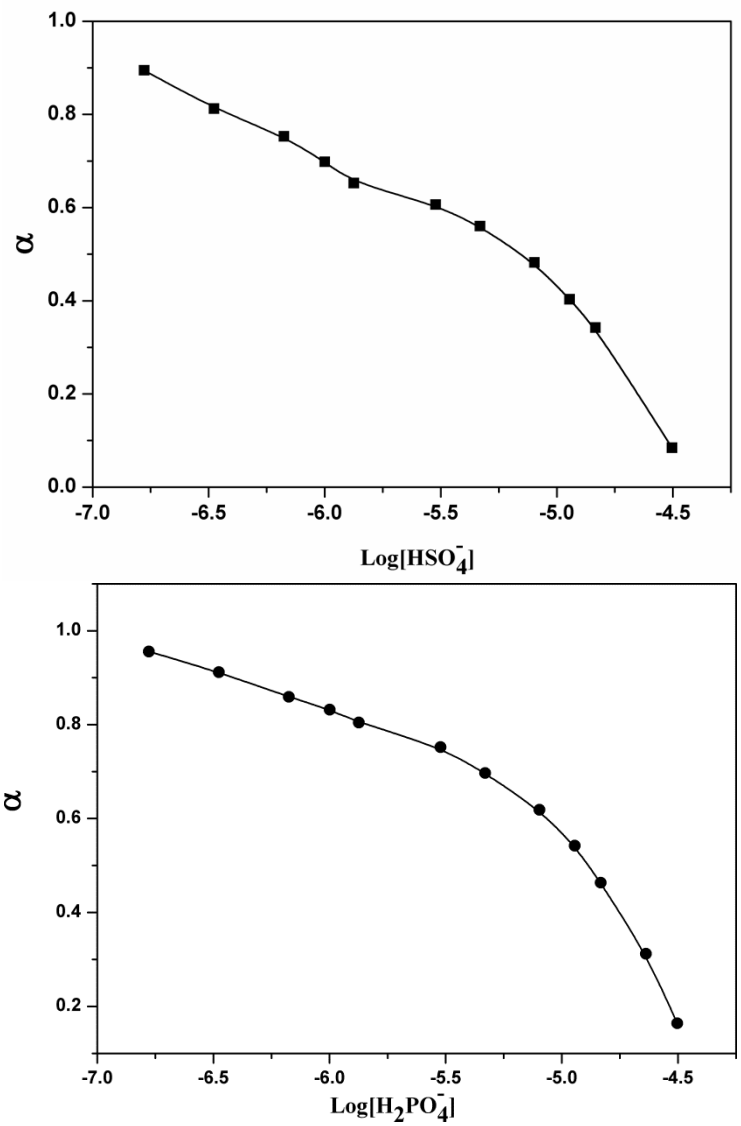


**Fig. S13** Response parameter values (**α**) as a function of the logarithm of $H_2SO_4^-$ and $HPO_4^-$ concentration.

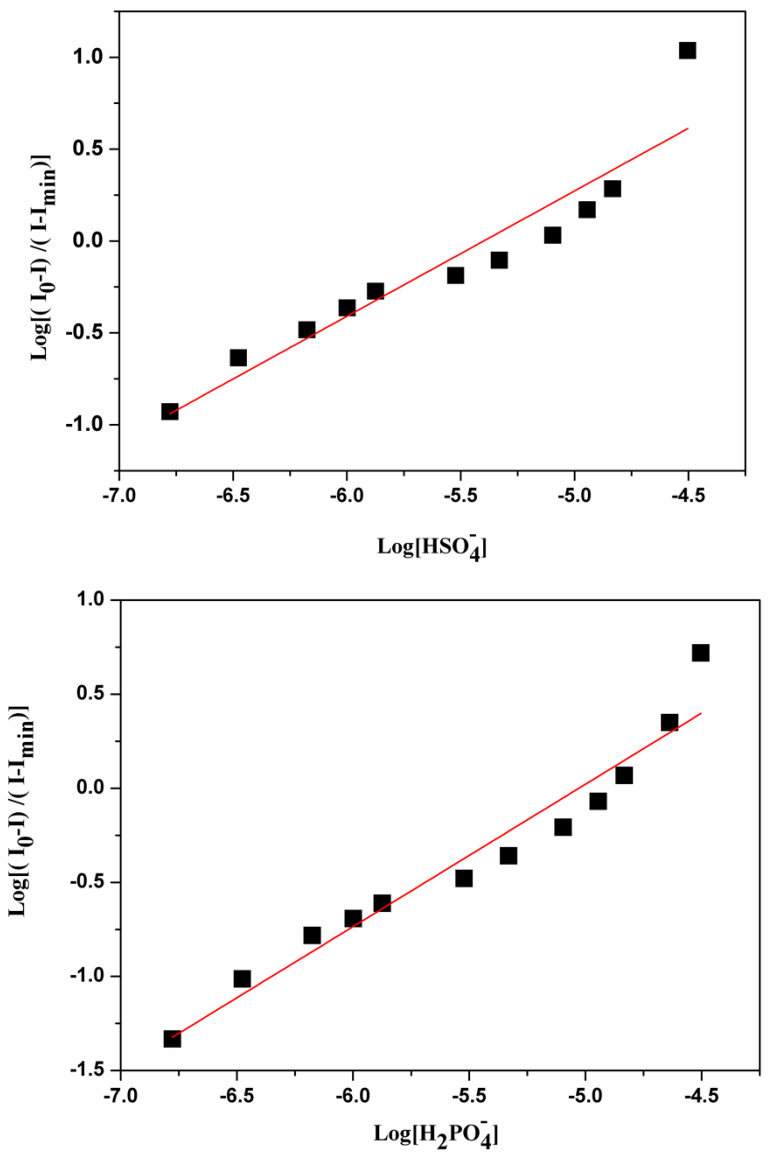


**Fig. S14** The double logarithm plot of the $Eu^{III}$ emission in the presence of increasing amounts of $HSO_4^-$ and $H_2PO_4^-$, and the corresponding linear fitting.

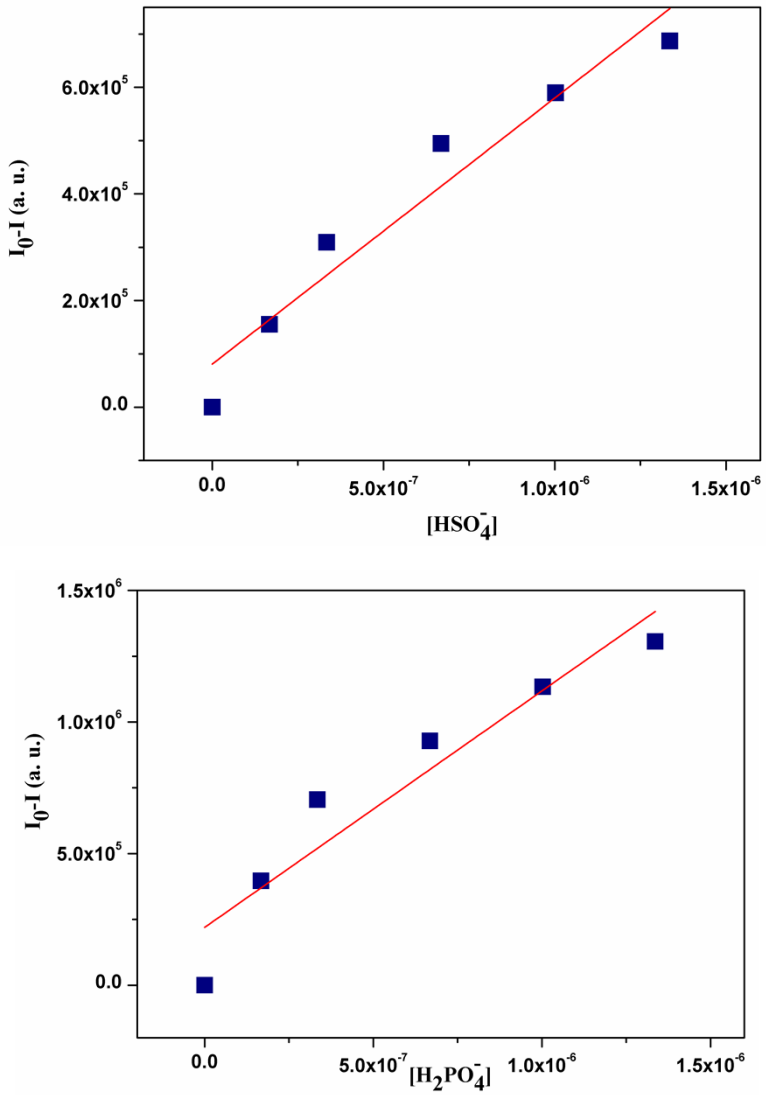


**Fig. S15** The changes of emission intensity (at 617 nm) of **$Eu_2PQC_6$** with different concentrations of $H_2PO_4^-$ and $HSO_4^-$ added, where $I_0$ and $I$ are the emission intensities of **$Eu_2PQC_6$** in the absence of $H_2PO_4^-$ and $HSO_4^-$ and at varying amounts of $H_2PO_4^-$ and $HSO_4^-$, respectively.

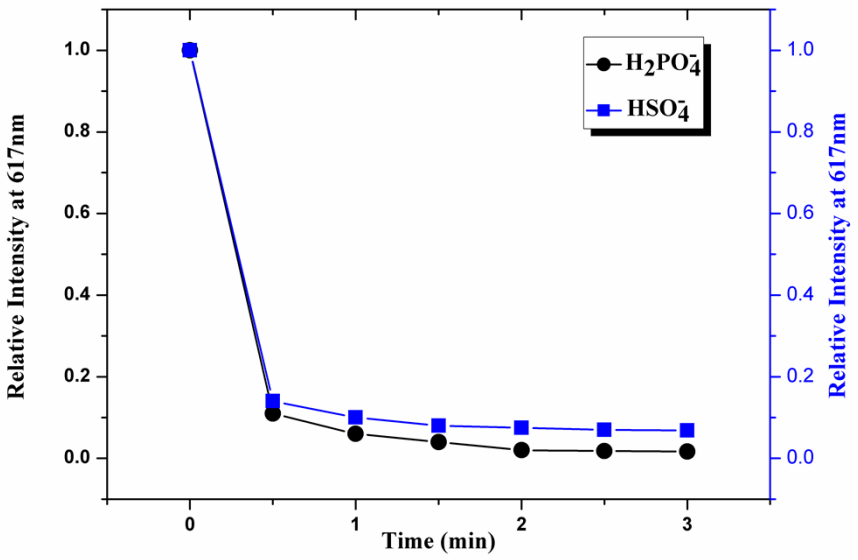


**Fig. S16** The respond time of $\mathbf{Eu_2PQC_6}$ to $H_2PO_4^-$ and $HSO_4^-$(3.0 equiv).

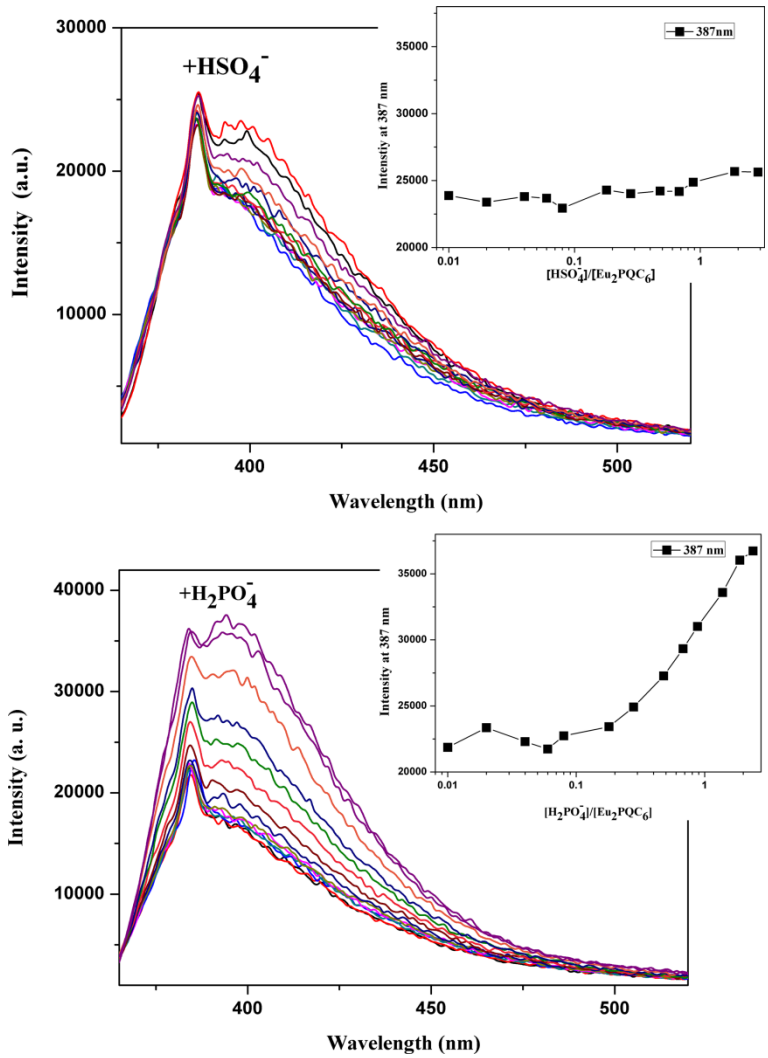


**Fig. S17** The changes in emission from PQC ligand upon addition of $H_2PO_4^-$ and $HSO_4^-$, respectively. Inset: intensity at 387 nm as a function of $H_2PO_4^-$ and $HSO_4^-$ concentration.

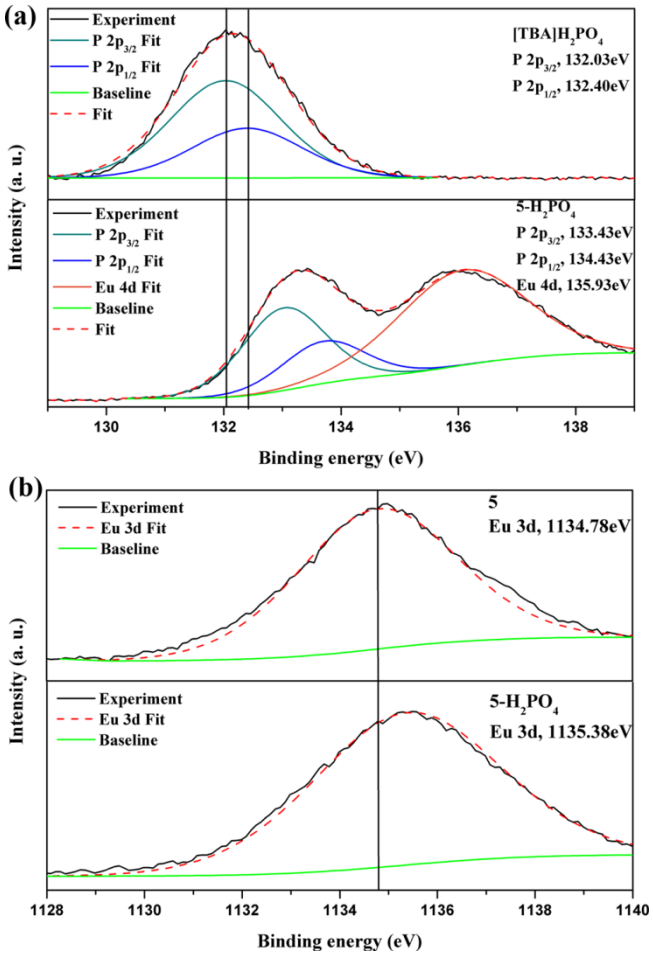


**Fig.S18** (a) P $2p_{1/2}$ and $2p_{3/2}$ spectra obtained for $[TBA]H_2PO_4$ and **5**-$H_2PO_4^-$ sample, (b) Eu $3d_{5/2}$ spectra obtained for **5** and **5**-$H_2PO_4^-$ sample, respectively.

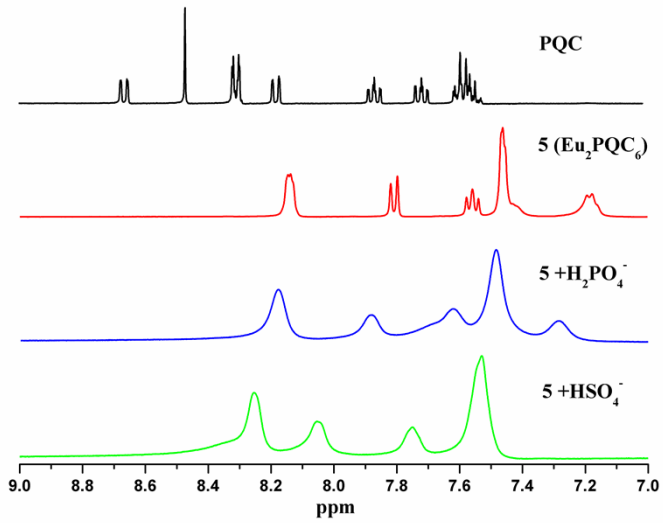


**Fig. S19** $^1$H-NMR spectra of PQC, **5**, **5** addition with 1.0 equiv of $H_2PO_4^-$ and $HSO_4^-$ in DMSO-$d_6$ solution.

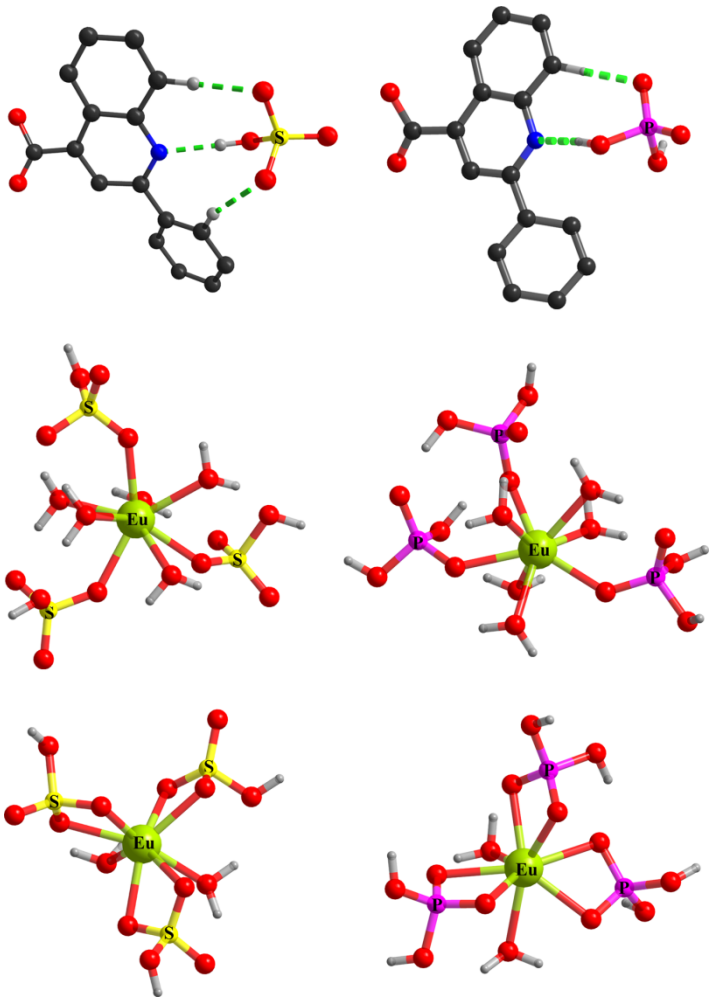


**Fig. S20** The optimized structures of investigated PQC-$HSO_4^-$/$H_2PO_4^-$ hydrogen-bonding interaction and Eu-$HSO_4^-$/$H_2PO_4^-$ coordination-bonding interaction by DFT method.

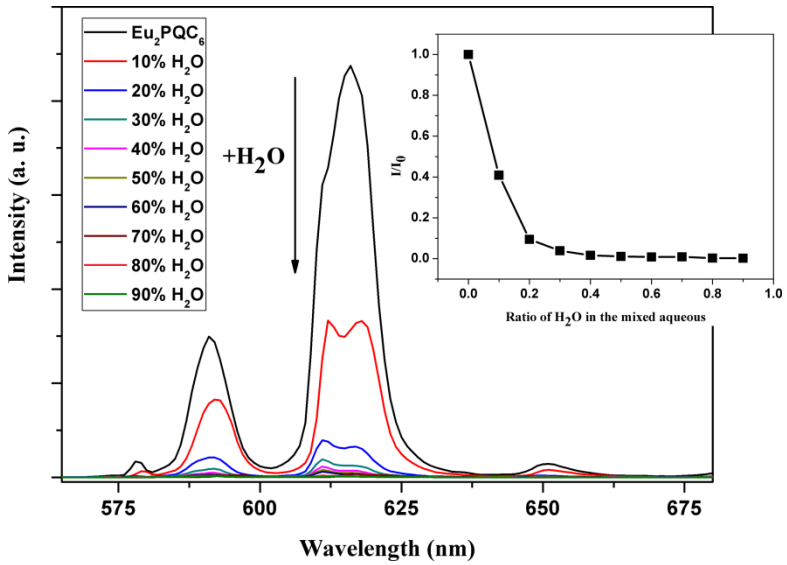


**Fig. S21** The evolution of the fluorescence emission of **$Eu_2PQC_6$** (50μM) in $H_2O$-DMSO solution ($\lambda_{ex}$ = 343 nm).

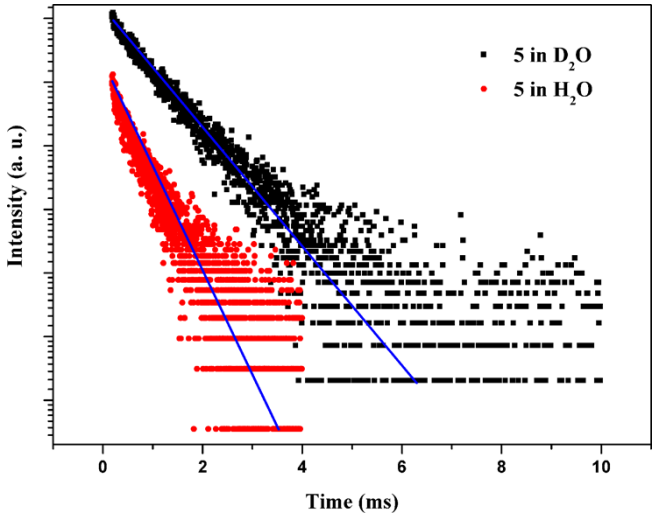


**Fig. S22** Luminescence decay curve excited at 343 nm at 77 K of **$Eu_2PQC_6$** (50 μM) in $D_2O$-DMSO (v/v =10:90) and $H_2O$-DMSO (v/v =10:90) solution, respectively.

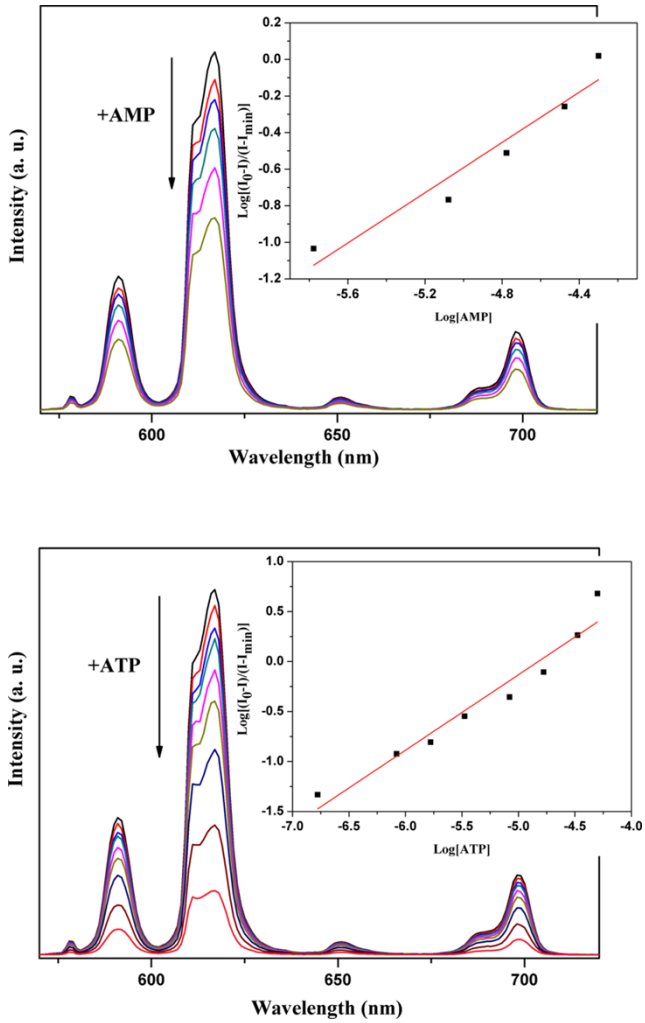


**Fig. S23** Emission spectra of **5** (16.7μM) against AMP and ATP in 10:90 (v/v) $H_2O$-DMSO solution. The inset shows the linear fit related to the binding constant determination.